

UNIVERSITY OF LATVIA
FACULTY OF PHYSICS AND MATHEMATICS



Gints Kučinskis

**THE STUDY OF NANOSTRUCTURED BULK
AND THIN FILM LiFePO_4 CATHODE
MATERIALS FOR LITHIUM-ION BATTERIES**

Summary of Doctoral Thesis

Submitted for the degree of Doctor of physics
Subfield of material physics

Rīga, 2015

The doctoral thesis was carried out at Institute of Solid State Physics, University of Latvia from 2012 to 2015.



LATVIJAS
UNIVERSITĀTE
ANNO 1919

IEGULDĪJUMS TAVĀ NĀKOTNĒ

This work has been supported by the European Social Fund within the project
“Support for Doctoral Studies at University of Latvia”
No. 2009/0138/IDP/1.1.2.1.2./09/TPIA/VIAA/004

The thesis contains introduction, 4 chapters, conclusions and reference list.

Form of the thesis: dissertation in physics, subfield of material physics

Supervisor: Dr. chem. Gunārs Bajārs,
senior researcher, head of the Laboratory of Solid State Ionics,
Institute of Solid State Physics, University of Latvia

Reviewers:

- 1) Guntars Vaivars, Dr. chem., senior researcher,
Faculty of Chemistry, University of Latvia;
- 2) Tomas Šalkus, Dr. phys., researcher, associated professor,
Faculty of Physics, Vilnius University;
- 3) Jānis Grabis, Dr. habil. sc. ing, director, head of Plasma Process
Laboratory, Institute of Inorganic Chemistry, Riga Technical University

The thesis will be defended at the public session of the Doctoral Committee of Physics, Astronomy and Mechanics, University of Latvia, at 15:00 on August 27, 2015 at Kengaraga 8, conference hall.

The thesis is available at the Library of the University of Latvia, Raiņa Blvd 19.

Chairman of the
Doctoral Committee: _____ Dr. habil. phys. Linards Skuja

Secretary of the Doctoral Committee: _____ Laureta Buševica

© University of Latvia, 2015
© Gints Kučinskis, 2015

ISBN 978-9934-18-043-3

ABSTRACT

In this work LiFePO_4 lithium ion battery cathode material and its thin films have been studied. The possibilities of improving electrochemical properties and rate capability of LiFePO_4 were analysed by optimizing the synthesis conditions and experimenting with reduced graphene oxide electron-conducting additive. LiFePO_4 thin films were obtained, their composition, structure, morphology and electrochemical properties were analysed. The model of sequential LiFePO_4 particle charge and discharge was analysed and improved in context of LiFePO_4 bulk material and thin films. The results give extensive understanding of lithium insertion and de-insertion processes taking place in LiFePO_4 cathode and demonstrates pre-requisites necessary for improving the rate capability of LiFePO_4 .

Keywords: Lithium ion batteries; LiFePO_4 ; cathode; thin films

CONTENTS

1. Introduction	5
1.1. Overview	5
1.2. Scientific Novelty of the Work	7
1.3. Aim and Objectives of the Work	7
2. Literature Review	8
2.1. Lithium Ion Battery	8
2.2. LiFePO_4 Lithium Ion Battery Cathode Material	8
2.3. Thin Film Technology	11
3. Experimental	12
3.1. LiFePO_4 Preparation	12
3.2. Structure, Composition and Morphology Characterization of the Prepared Materials	13
3.3. Thin Film Deposition	13
3.4. Analysis of Thin Film Composition, Structure and Morphology ...	13
3.5. Electrochemical Measurements	14
3.6. The Study of Sequential LiFePO_4 Grain Charge and Discharge by X-Ray Absorption Spectroscopy	15
4. Results and Discussion	16
4.1. LiFePO_4 Bulk Material and $\text{LiFePO}_4/\text{C}/\text{rGO}$ Nanocomposite	16
4.2. Electrochemical Properties of LiFePO_4 Thin Films	19
4.2.1. Thin Films Deposited by Pulsed Laser Deposition	19
4.2.2. Thin Films Deposited by Magnetron Sputtering	22
4.3. The Analysis of Sequential LiFePO_4 Particle Charging and Discharging	23
4.3.1. In-situ XAS Measurements of LiFePO_4 Bulk Material	23
4.3.2. Sequential Particle Charging and Discharging in LiFePO_4 Thin Films	24
Conclusions	28
Theses	30
References	31
Approbation of the Work	35
Scientific Projects	35
Scientific Conferences	35
International Conferences	35
Local Conferences	36
Scientific Schools	36
Scientific Publications	37
SCI Publications	37
Other Publications	37
Acknowledgements	38

1. INTRODUCTION

1.1. Overview

Lithium ion battery is one of the most popular rechargeable battery types. LiFePO_4 is a lithium ion battery cathode material which was initially forecast to be a good candidate for low power lithium ion batteries [1]. However, due to several advances in LiFePO_4 preparation, mostly involving the use of electron-conducting additives [2] and grain size reduction [3], LiFePO_4 has become one of the most promising high power lithium ion battery electrode materials. LiFePO_4 has high charge capacity, excellent stability [4] and outstanding cyclability [5], which is ensured by the small volume changes that LiFePO_4 undergoes during lithium insertion and extraction [1, 6]. Although LiFePO_4 is one of the most researched lithium ion battery cathode materials, there are still several uncertainties about its fundamental working principles [7]. The possibilities of improving its physico-chemical properties are also still being actively studied [7–11].

Further improvement of LiFePO_4 rate capability (the ability of a LiFePO_4 cathode to rapidly insert and extract lithium) can be a determining factor for the use of LiFePO_4 in mass-produced lithium ion batteries. One of the most simple ways of improving LiFePO_4 rate capability is improving its low electronic conductivity (10^{-9} S/cm [12–14]) by using electron conducting additives. For this purpose carbon additives are often used [15–22]. Due to recent progress [23], graphene is becoming more researched and more readily available. Graphene has one of the largest room temperature electronic conductivities [24]. Although it has previously been shown that graphene can be used as an electron-conducting additive for lithium ion battery materials with good results [9, 25–44], it is still not completely understood what grain structure of LiFePO_4 – graphene or reduced graphene oxide (rGO) composites is more desirable [45]. Some studies suggest that the most effective structure in terms of improved electrochemical properties is a homogenous mix of LiFePO_4 particles and rGO sheets [26–28, 33–35, 46]. However, other researchers consider the structure with rGO sheets wrapping LiFePO_4 grains to be the most optimal one [9, 29, 31]. Some studies claim that LiFePO_4 particles anchored on rGO sheets and possibly chemically bonded to the rGO sheets is the best LiFePO_4 – rGO composite in terms of rate capability and other electrochemical properties [30]. Due to different GO and LiFePO_4 preparation methods used, a direct comparison between the individual studies is not possible. In this work LiFePO_4 – rGO nanocomposites with various grain structures have been obtained. The connection between the grain structure and physico-chemical properties of the composite has been studied.

In a broader sense, a precise understanding of lithium insertion and extraction in LiFePO_4 can provide a significant contribution in improving its rate capability and other electrochemical properties [47]. During charge and discharge lithium rich and lithium poor phase can exist in a Li_xFePO_4 grain simultaneously [48–51], and there are several models that describe how the two phases can be distributed within the single LiFePO_4 grain [1, 52–56]. There can also be lithium rich and lithium poor grains in a Li_xFePO_4 electrode at an equilibrium state [53, 54, 57]. However, until now it has not been convincingly demonstrated how the lithium is distributed in Li_xFePO_4 electrode during the charge and discharge. This work attempts to demonstrate it by using *in-situ* X-ray absorption spectroscopy imaging.

Several papers that are studying sequential LiFePO_4 particle charge and discharge by conducting electrochemical measurements have recently been published [58–61]. Sequential lithiation and de-lithiation of LiFePO_4 grains is made possible by the non-monotonic lithium chemical potential – lithium content x in Li_xFePO_4 dependence [47, 59], LiFePO_4 standard electrode potentials varying with grain sizes [62, 63] and due to the fact that there is not equally good electronic contact between all LiFePO_4 grains and the current collector [59]. LiFePO_4 thin film is a unique system for use in fundamental electrochemical experiments. However, it has not been done before. In a thin film it is not necessary to use electron-conducting additives or binders, therefore creating a homogenous system in which a significant number of grains are in direct contact with both the current collector and electrolyte. The analysis of a material with this unique grain structure can provide a deep understanding of various electrochemical phenomena, especially about the non-vanishing voltage hysteresis that has been based on the assumption of sequential LiFePO_4 particle charge and discharge [59, 60].

While providing a unique grain structure, LiFePO_4 thin films also have advantages connected with practical applications. Thin film electrodes can easily be obtained on substrates of various shapes. Additionally the energy density of thin film battery electrodes is higher than many conventional lithium ion battery electrodes [64]. There are several studies that demonstrate the possibility of creating a thin film lithium ion battery [65–67]. Due to the small volume changes during lithiation and de-lithiation (approximately 5 % [6]), LiFePO_4 is an excellent candidate for use in all-solid thin film lithium ion batteries. In this work LiFePO_4 thin film deposition with pulsed laser deposition and magnetron sputtering has been studied by analysing physico-chemical properties of the obtained thin films and the possible optimization of the deposition techniques.

1.2. Scientific Novelty of the Work

In this work LiFePO_4 lithium ion battery cathode and its physico-chemical properties have been extensively studied. The little studied influence of preparation technique and grain structure on physico-chemical properties of LiFePO_4 – rGO has been researched. $\text{LiFePO}_4/\text{C}/\text{rGO}$ material that is an excellent candidate for high power and high capacity lithium ion batteries has been prepared. Thin films with one of the largest charge capacities reported in literature have been deposited. For the first time several electrochemical phenomena characteristic to the sequential grain-by-grain charging and discharging have been studied in the unique grain structure of LiFePO_4 thin films. Sequential charging and discharging of LiFePO_4 bulk electrode particles has been demonstrated. The unique combination of the experimental methods used in this work provides experimentally based knowledge that can significantly contribute to further LiFePO_4 and other lithium ion battery material development and their physico-chemical property optimization.

1.3. Aim and Objectives of the Work

The aim of this work is to expand the understanding of working principles of LiFePO_4 lithium ion battery cathode material. The obtained knowledge would provide a potential to increase the rate of lithium insertion and extraction of LiFePO_4 and potentially other two phase lithium insertion and extraction cathodes.

In order to achieve the aim of this work, following objectives have been put forward:

- Obtain $\text{LiFePO}_4/\text{C}/\text{reduced}$ graphene oxide composites and analyse their physico-chemical properties in connection with their preparation technique
- Deposit LiFePO_4 thin films and analyse their physico-chemical properties
- Experimentally analyse sequential grain charging and discharging in LiFePO_4 bulk material
- Verify the conformity of sequential charging and discharging model for LiFePO_4 thin films with the help of low and very low current galvanostatic experiments

2. LITERATURE REVIEW

2.1. Lithium Ion Battery

A Lithium Ion Battery is a device that can convert the chemical energy stored in its active materials directly into electric energy by using electrochemical oxidation – reduction reactions [68]. It is composed of one or more electrochemical cells that are connected in parallel, series or in a mixed circuit. Electrochemical cell is a basic unit of a battery, it is composed of an anode or a negative electrode, a cathode or a positive electrode and electrolyte – an ionic conductor and electronic insulator located between the two electrodes. Lithium ion battery is based on the transport of lithium ions between the cathode and the anode.

Mostly owing to the previous research of lithium ion conducting electrodes [69–71], in 1991 the first mass produced lithium ion battery was introduced to the market by Sony [72]. Due to several improvements, the capacity of the advanced lithium ion batteries has almost tripled [73]. Currently lithium ion batteries are being used in portable electronics, power tools and hybrid and electric vehicles [74, 75]. Although lithium ion battery is one of the most popular battery types in the world, serious advancements in the technology itself is still required. Most of the progress made in the field of lithium ion batteries is based on material research [76, 77].

2.2. LiFePO_4 Lithium Ion Battery Cathode Material

Phosphate compounds, such as LiFePO_4 , are a relatively new class of lithium ion battery cathode materials. LiFePO_4 was first reported in 1997 [1]. These compounds have orthorhombic crystal lattice – the structure is shown in Fig. 2.1. In mineralogy this structure is called triphylite. Lithium ions in LiFePO_4 are located in a one dimensional chains or one dimensional channels in [010] crystallographic direction.

Experiments have proven that in comparison with other transition metals which are used in LiMPO_4 (M – transition metal), best electrochemical properties are shown by M = Fe [11]. LiFePO_4 is also the cheapest to produce from the viewpoint of the cost of raw materials. LiFePO_4 is the least toxic when compared with other LiMPO_4 materials [79]. In

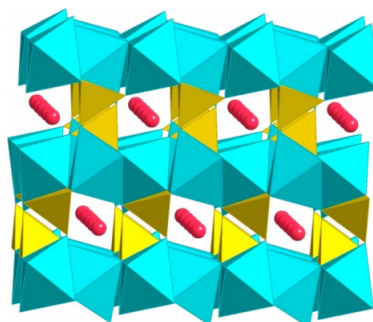


Fig 2.1. LiMPO_4 structure, transition metal M ions are blue, P ions are yellow, Li ions are red [78]

addition to that, LiMPO_4 is also a chemically stable class of materials – the risk of thermal runaway for batteries with LiMPO_4 cathodes is very low. Due to the small volume changes during cycling the cyclability is very good. This has promoted the use of LiFePO_4 in transportation applications – electric and hybrid vehicles [80, 81]. The electronic conductivity of LiFePO_4 is 10^{-9} S/cm [12–14], and it is several orders of magnitude lower than the electronic conductivities of most other popular cathode materials. The experimentally determined effective chemical diffusion coefficient of lithium in LiFePO_4 is $10^{-10} - 10^{-18}$ cm^2/s , although it depends on the lithium stoichiometry (state of charge) of LiFePO_4 [12, 82–84].

One of the most important parameters characterizing LiFePO_4 is its rate capability or the ability to rapidly insert and extract lithium from the material. Often carbon electron-conducting additives are used in order to improve the rate capability of LiFePO_4 [15–22]. They not only improve the rate capability but also allow to avoid impurity phases and to decrease the LiFePO_4 grain size [11]. Other ways of improving the rate capability is decreasing the grain size by modifying the synthesis [85], coating with lithium ion conducting additives [86] and preparing LiFePO_4 composites with other lithium insertion and extraction materials [87, 88].

Due to recent research advances [23], graphene is becoming more researched and more readily available. Graphene has one of the highest room temperature electronic conductivities [24]. Usually because of the relatively simple preparation and its hydrophilicity graphene oxide (GO) is used in the preparation of graphene composites. GO is usually reduced to form reduced graphene oxide (rGO) after the initial mixing step. Although it has previously been shown that graphene can successfully be used as an electron-conducting additive in lithium ion battery materials [9, 25–44], it is still not completely understood what grain structure of LiFePO_4 – graphene or reduced graphene oxide (rGO) composites is more desirable [45]. Some studies suggest that the most effective structure in terms of improved electrochemical properties is a homogenous mix of LiFePO_4 particles and rGO sheets [26–28, 33–35, 46]. However, other researchers consider the structure with rGO sheets wrapping LiFePO_4 grains to be the most optimal one [9,29,31]. Some studies claim that LiFePO_4 particles anchored on rGO sheets and possibly chemically bonded to the rGO sheets is the best LiFePO_4 – rGO composite in terms of rate capability and other electrochemical properties [30]. Due to different GO and LiFePO_4 preparation methods used, a direct comparison between the individual studies is not possible.

According to the Gibbs' phase rule and the LiFePO_4 galvanostatic charge and discharge curves, at low lithium concentrations in Li_xFePO_4 electrode a solid solution $\text{Li}_\beta\text{FePO}_4$ (β – positive, close to 0) is formed. Similarly at high lithium concentrations $\text{Li}_{1-\alpha}\text{FePO}_4$ (α – positive, close to 0) is formed. However, at intermediate lithium concentrations ($\beta < x < 1 - \alpha$) a mixture of both phases can be observed – a two-phase system is formed [49–51]. The boundary at which Li_xFePO_4 transforms from solid solution to a two-phase system or from the two-phase system to solid solution depends not only on the temperature but also on

the particle size, as reducing particle size leads to an increased surface area–mass ratio and therefore increases the relative amount of energy necessary for the creation of a two phase interface [62, 89]. Additionally the equilibrium potential of LiFePO_4 also depends on the particle size [62, 89–91].

A chemical potential of lithium for a single particle is shown in Fig. 2.2. Chemical potential μ and Gibbs' free energy G can be related via x – the amount of lithium in Li_xFePO_4 ($0 < x < 1$):

$$\frac{\partial G}{\partial x} = \mu, \quad (2.1.)$$

The chemical potential of lithium μ in LiFePO_4 is connected with the electric potential E of LiFePO_4 :

$$E = -\frac{\mu}{e} + E_0, \quad (2.2.)$$

where the constant e – elementary charge, E_0 – standard electrode potential. It is assumed that during a galvanostatic low current experiment Li chemical potential follows the red curve seen in Fig. 2.2., as the lithium content in $\text{Li}_\beta\text{FePO}_4$ solid solution increases. At some point the separation of lithium rich $\text{Li}_{1-\alpha}\text{FePO}_4$ phase and lithium poor $\text{Li}_\beta\text{FePO}_4$ phase occurs, and therefore a rapid decrease of the lithium chemical potential takes place. By inserting additional lithium in the two phase $\text{Li}_\beta\text{FePO}_4/\text{Li}_{1-\alpha}\text{FePO}_4$ material the amount of both phases changes but lithium concentration within these phases remains constant, therefore the chemical potential remains constant until the moment when the electrode has reached overall stoichiometry $\text{Li}_{1-\alpha}\text{FePO}_4$. At this point the $\text{Li}_\beta\text{FePO}_4$ phase is not present any more, and further insertion of lithium changes the stoichiometry of $\text{Li}_{1-\alpha}\text{FePO}_4$. Therefore according to Gibbs' phase rule the chemical potential increases again. In non-equilibrium conditions chemical potential – concentration curve can be different from the one shown in Fig. 2.2. [47].

In a typical LiFePO_4 bulk material electrode there are around 10^{10} LiFePO_4 grains. Recent *ex-situ* studies show that lithium is not being inserted simultaneously in all LiFePO_4 grains therefore leading to sequential particle-by-particle charging and discharging behaviour [53, 54, 57]. There are several electrochemical phenomena associated with sequential LiFePO_4 lithiation and de-lithiation [58, 59,

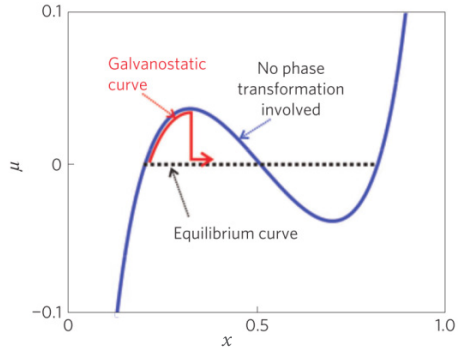


Fig. 2.2. Chemical potential of lithium versus the amount of lithium in Li_xFePO_4 for a single particle [59]

61, 92, 93]. One of such phenomena with the most far-reaching consequences is the non-vanishing voltage hysteresis of LiFePO_4 [59].

In the study of non-vanishing voltage hysteresis M. Gaberscek et al. demonstrate that even by performing charge and discharge experiments at an extremely slow C/1000 rate ($C = 170 \text{ mA/g}$), there is still a 20 mV difference between the charge and discharge voltage plateaus for a LiFePO_4 powder electrode [59]. Such hysteresis has a thermodynamic and not kinetic origin. It can be explained with the help of the non-monotonic shape of lithium chemical potential – concentration curve (Fig. 2.2.). By discharging the LiFePO_4 electrode, LiFePO_4 grains sequentially proceed through the maximum of the red (galvanostatic discharge) curve in Fig. 2.2. As the number of LiFePO_4 grains in the electrode is extremely large and the individual grains proceed through the chemical potential peak sequentially, instead of a plateau at the equilibrium position a plateau at the local single particle chemical potential maximum is observed. A symmetrical process takes place during the de-lithiation of LiFePO_4 therefore leading to the non-vanishing voltage hysteresis of around 20 mV.

2.3. Thin Film Technology

A thin film is a thin layer of material which has been obtained by depositing single atoms, molecules or ions [94]. A thin film is different from a thick film, which is obtained by reducing the size of a thick material or depositing readily-made grains or big clusters of atoms, molecules and ions.

There are chemical and physical thin film deposition techniques. Physical techniques include mechanical, electromechanical or thermodynamic processes, while chemical thin film deposition techniques usually involve a liquid precursor that forms a thin solid film as a result of a chemical reaction. The most popular physical thin film deposition techniques are physical vapour deposition (resistive, inductive, electron beam, pulsed laser, arc-discharge, etc.), sputtering techniques (cathode, magnetron, direct current, alternating current, impulse, etc.) and electrodynamic deposition.

Pulsed laser deposition (PLD) is based on a target located in a vacuum chamber being irradiated with a high energy pulsed laser. As a result of it the target atoms are being excited. Target ablation, surface exfoliation and plasma formation take place [95]. The products of pulsed laser – target interaction form a directed flow of particles towards the substrate. Part of the particles are deposited on the substrate and form a thin film. This technique is relatively easy to optimize and therefore is very popular for scientific purposes.

Magnetron sputtering is another popular physical vapour deposition technique. Contrary to PLD, magnetron sputtering can easily be used to coat large surfaces. The technique is based on collisions between an inert gas and a target, which is made either from a pressed powder or a monolithic metal or alloy.

3. EXPERIMENTAL

3.1. LiFePO₄ Preparation

LiFePO₄/C was prepared via solution synthesis from LiH₂PO₄ and FeC₂O₄·2H₂O. The reactants were used in molar ratio 1:1. Citric acid (C₆H₈O₇) was added as a source of additional carbon. Citric acid constituted 16 % of the total weight of the reactants. The reactants were stirred in a deionized water, the water was slowly evaporated, as the temperature of the magnetic stirrer's hotplate was 100 °C. After drying the reactants were grinded and heated at 350 °C in argon – hydrogen gas flow, the amount of hydrogen in the gas was 5 vol.%. The obtained precursor was then milled and sintered for 5 h at 700 °C in Ar / 5 vol.% H₂ flow.

LiFePO₄/C/rGO composite was obtained in three different ways. 3 wt.% graphene oxide (GO, Bluestone, sheet size 1–20 μm) was added at various steps of the aforementioned LiFePO₄/C synthesis. The samples are numbered accordingly:

- LFP/C/rGO (1) – GO added during the preparation of precursor,
- LFP/C/rGO (2) – GO added to the precursor before sintering,
- LFP/C/rGO (3) – GO added to LiFePO₄/C, the thermal reduction of GO took place afterwards with the sample being heated at 700 °C for 3.5 h in Ar / 5 vol.% H₂ flow.

The addition of GO always took place by stirring GO with the rest of the reactants in 40 ml deionized water followed by evaporation of the water as described before.

The LiFePO₄ target for PLD was prepared in a way similar to the solution synthesis described above. LiH₂PO₄ and Fe(NO₃)₃·9H₂O were used in a molar ratio 1:1. The reactants were stirred in 60 ml deionized water while slowly evaporating the water. The temperature of the magnetic stirrer's hot-plate was 150 °C. When enough water was evaporated to form a gel, the temperature of the hot-plate was reduced to 100 °C. The obtained powder was then grinded and heated in Ar / 5 vol.% H₂ flow for 4 h at 300 °C. After cooling down the LiFePO₄ precursor was grinded and isostatically pressed into tablets with 400 kN force. The diameter of the tablet was 15 mm, height – 3 mm. The tablets were then sintered at 500 °C for 10 h in Ar / 5 vol.% H₂ flow. After synthesis the obtained LiFePO₄ was grinded again. PLD target was prepared by isostatically pressing the grinded LiFePO₄ powder into a tablet with a 15 mm diameter and 3 mm height by using 800 kN force. In order to avoid the splitting of the target during deposition, the prepared tablet was heat-treated at 600 °C for 2 h in Ar / 5 vol.% H₂ flow. The heating rate was always 5 °C/min. The surface of the prepared target was polished with a fine sandpaper before the deposition.

3.2. Structure, Composition and Morphology Characterization of the Prepared Materials

The synthesized powders were analysed by using X-ray diffraction (XRD, Cu K_α radiation) and Raman spectroscopy. LiFePO₄ intended for use as a PLD target was additionally characterized by inductively coupled plasma optical emission spectroscopy (ICP-OES). LiFePO₄/C and LiFePO₄/C/rGO were additionally characterized by scanning electron microscopy (SEM), and carbon content was determined via thermogravimetric analysis (TGA). Specific surface area was studied with nitrogen adsorption measurements followed by Brunauer, Emmett and Teller (BET) analysis.

3.3. Thin Film Deposition

ArF excimer laser with a wavelength of 248 nm was used for LiFePO₄ thin film deposition by PLD. The energy of the laser beam in front of the lens of the vacuum chamber was 70 – 90 mJ, the area of the target irradiated by the laser – 4.5 mm². Laser frequency – 5 Hz, pulse length – 25 ns. The target material was LiFePO₄ tablet that was prepared as described before. The initial vacuum in the vacuum chamber was 3·10⁻⁶ mBar. The chamber was then filled with argon to a pressure of 0.2 mBar, gas flow – 3 sccm/s. During the thin film deposition the target rotation speed was 0.5 Hz. Before the thin film deposition the target was pre-ablated with 600 laser pulses. During the thin film deposition the substrate temperature was 500 – 530 °C. Thin films were deposited on Nb doped SrTiO₃ (Nb:STO) monocrystals, Nb content – 0.5 wt.%, polished from one side, crystallographic orientation (100), size: 5 x 5 mm.

In order to obtain LiFePO₄ thin films by magnetron sputtering a magnetron sputtering device made by *Sidrabe Inc.* was used in radio frequency mode. Frequency: 13.56 MHz, power: 300 W. Target was prepared by pressing LiFePO₄ powder (*Linyi Gelon New Battery Materials Co.*) with 7 t weight (3.9 MPa pressure). The diameter of the target – 15 cm, distance between the target and substrate – 15 cm. Before deposition a pressure of 5·10⁻⁵ mBar was obtained in the vacuum chamber. Argon was used as a sputtering gas, the target was pre-sputtered for at least 10 min. At some cases substrate was heated to 500 °C. Thin films were deposited on stainless steel, silicon monocrystals and glass substrates. In some cases thin film recrystallization for 1 h at 600 °C in Ar was performed.

3.4. Analysis of Thin Film Composition, Structure and Morphology

The structure of LiFePO₄ thin films obtained by magnetron sputtering was analysed by XRD (Cu K_α radiation). Morphology was studied by SEM.

Thickness was determined by a profilometer, thin films deposited on a silicon monocrystal were used for this purpose.

The structure of LiFePO_4 thin films deposited by PLD was studied by using XRD and grazing incidence XRD (Cu K_α radiation). The composition was analysed by ICP-OES. Thin film stoichiometry on the surface and in the bulk of the thin film was analysed by secondary ion mass spectroscopy (SIMS) by using 15 keV Ga^+ ion gun. Thin film surface was studied by X-ray photoelectron spectroscopy (XPS), the spectra were obtained in a vacuum chamber with a pressure under $2 \cdot 10^{-10}$ Torr by using Al K_α X-rays with 1486.6 eV energy. Thin film surface was analysed by SEM and atomic force microscopy (AFM). AFM was used in a contact mode, silicon needle with a radius smaller than 10 nm was used. Thin film thickness was determined by breaking the thin film and analysing the cross-section by SEM or by a focused ion beam (FIB) – gallium ions were used to etch a part of the thin film, the cross-section was then studied by SEM.

3.5. Electrochemical Measurements

LiFePO_4/C , $\text{LiFePO}_4/\text{C}/\text{rGO}$ and LiFePO_4 thin films deposited by magnetron sputtering were measured in a Swagelok-type two electrode electrochemical cells with a metallic lithium counter electrode that was at the same time also used as a reference electrode. Bulk material electrodes were prepared by mixing the active cathode material with acetylene black and polyvinylidene fluoride (PVDF) in *n*-methyl-2-pyrrolidone in a mass ratio 75 : 15 : 10. The obtained slurry was ball-milled for 20 min and then coated on an aluminium foil. The diameter of the electrodes used – 10 mm. 1 M LiPF_6 in ethylene carbonate (EC) and dimethyl carbonate (DMC) in volume ratio 1:1 was used as an electrolyte. *Whatman GF/F* glass microfiber separator was used. Electrochemical impedance spectroscopy was carried out in a cell containing 1 M LiClO_4 in propylene carbonate as an electrolyte. Electrochemical cells were assembled in an argon-filled glove box. Electrochemical measurements were carried out with potentiostat *Voltalab PGZ-301* and *Solartron 1287A* in combination with frequency analyser *Solartron 1255*.

LiFePO_4 thin films deposited by PLD were measured in Swagelok-type two electrode electrochemical cells. Metallic lithium was used both as a counter and reference electrode. The electrolyte was 1 M LiPF_6 in EC and diethylene carbonate (DEC) in volume ratio 1:1. *Celgard 2500* polypropylene (PP) separator was used. Electrochemical cells were assembled in an argon-filled glove box with O_2 and H_2O content lower than 1 ppm. Electrochemical measurements were performed by using potentiostats *Voltalab PGZ-301*, *Voltalab PGZ-402*, *Autolab PGSTAT101* and *Solartron 1287A* in combination with frequency analyser *Solartron 1255*.

3.6. The Study of Sequential LiFePO₄ Grain Charge and Discharge by X-Ray Absorption Spectroscopy

The LiFePO₄ electrodes for X-ray absorption measurements were prepared by mixing LiFePO₄ (*M.T.I. Corp.*), *Super P* and PVDF in n-methyl-2-pyrrolidone in mass ratio 75 : 15: 10. The obtained slurry was coated on a 15 μm thick aluminium foil, electrode diameter was 10 mm. Before assembling the cell the electrodes were dried for 20 h in vacuum furnace at 100 °C. Electrochemical measurements were done in a two electrode configuration with metallic lithium foil being used as the counter electrode and at the same time also as a reference electrode. 1 M LiPF₆ in EC and DEC in volume ratio 1:1 was used as an electrolyte. *Celgard 2500* PP separator with a thickness of 25 μm was used. Electrochemical cells were assembled in an argon-filled glove box with O₂ and H₂O content lower than 1 ppm. A custom made electrochemical cell was used. Beryllium monocrystals were used as X-ray transparent windows.

X-ray absorption experiments were performed at BAMline beam line at BESSY II synchrotron in Berlin, Germany. X-ray absorption near edge structure (XANES) of LiFePO₄ was studied in an imaging mode in the Fe K-edge (7112 eV) energy region before, during and after charge and discharge of LiFePO₄. The energies used were 7080 – 7150 eV. Fe foil was used as a reference. Fe oxidation state was determined based on the shift of the Fe K-edge. Lithium rich Li_xFePO₄ contains mostly Fe²⁺ and lithium poor Li_xFePO₄ contains mostly Fe³⁺, therefore it is possible to evaluate lithium content in Li_xFePO₄ by determining the Fe oxidation state.

In order to obtain a monochromatic beam, double multilayer monochromator (DMM) and Si (111) double crystal monochromator (DCM) were used in series. Behind the electrochemical cell an X-ray luminescent screen was placed turning X-rays into visible light. The light from the luminescent screen was focused on a CCD (charge-coupled device) camera. A more detailed information on BESSY II BAMline beamline can be obtained in references [96] and [97].

4. RESULTS AND DISCUSSION

4.1. LiFePO₄ Bulk Material and LiFePO₄/C/rGO Nanocomposite

X-ray diffraction (XRD) analysis displays all peaks characteristic to the orthorhombic LiFePO₄ crystal lattice and Pnma space group, no impurities have been observed. Raman spectroscopy shows carbon D and G bands located at 1350 cm⁻¹ and 1600 cm⁻¹ respectively. No significant differences in Raman spectra can be observed between samples with and without rGO, therefore it can be concluded that carbon coating of LiFePO₄ creates a stronger signal than rGO. This is in agreement with the notion of very thin rGO sheets – because of the small thickness of one or few rGO layers the signal from rGO is very weak. TGA shows that LiFePO₄/C consists of 1.1 % carbon and confirms that LiFePO₄/C/rGO additionally contains almost 3 % rGO.

SEM images of LiFePO₄/C and LiFePO₄/C/rGO are shown in fig. 4.1. The grain size is approximately 100 – 700 nm, the obtained powders are noticeably porous (see fig. 4.1. a and b). The BET surface area is not sensitive to rGO, therefore it is similar to all prepared composites – approximately 30 m²/g. The average pore volume is 56 mm³/g.

The observation of single and few layer graphene in SEM is complicated, and often advanced SEM equipment is necessary, as one or few layer graphene can be nearly transparent for high energy electron beams [98,99]. Nevertheless, rGO sheets have been observed in all prepared LiFePO₄/C/rGO samples. In LiFePO₄/C/rGO (1) where GO was added at the first step of the synthesis rGO layers that have wrapped LiFePO₄ particles can be observed (see fig. 4.1. c). There are also LiFePO₄ particles that appear to be anchored on rGO sheets. The grain structure of LiFePO₄/C/rGO (2) and LiFePO₄/C/rGO (3) is significantly different than that of the sample LiFePO₄/C/rGO (1). Samples LiFePO₄/C/rGO (2) and LiFePO₄/C/rGO (3) have been obtained by adding GO in the second synthesis step and after LiFePO₄/C synthesis respectively. rGO sheets are mixed with LiFePO₄/C agglomerations (fig. 4.1. d). If wrapping of LiFePO₄/C has been observed, the rGO layers have wrapped parts of LiFePO₄ grain agglomerations and not individual LiFePO₄ grains. The grain structure where small LiFePO₄/C particles have been anchored on rGO sheets were not observed in composites LiFePO₄/C/rGO (2) and LiFePO₄/C/rGO (3).

The presence of rGO in LiFePO₄/C/rGO composite has caused an increase of the already high rate capability of LiFePO₄/C (see fig. 4.2.). The capacity of LiFePO₄/C/rGO (1) composite at 0.1 C current is up to 163.5 mAh/g. The rGO-wrapped LiFePO₄/C grains in sample LiFePO₄/C/rGO (1) have also provided significant rate capability improvements. The galvanostatic discharge

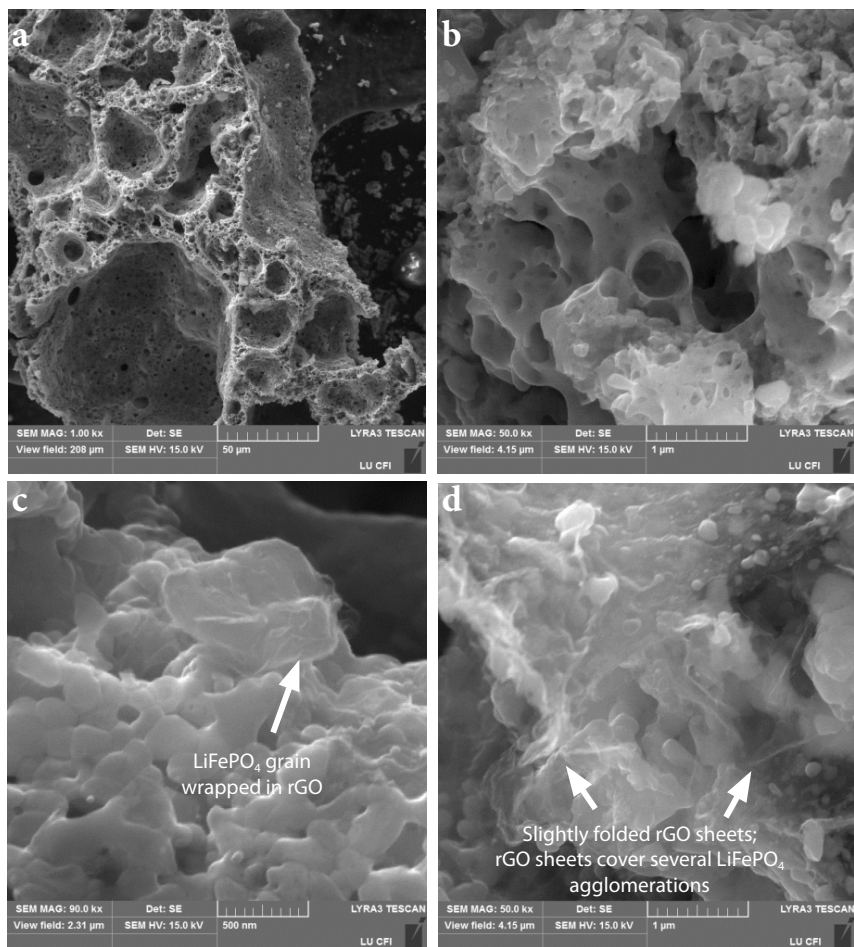


Fig. 4.1. SEM images: (a) and (b) LiFePO₄/C and its pores; (c) LiFePO₄/C/rGO (1) image with LiFePO₄/C grain wrapped in rGO; (d) LiFePO₄/C/rGO (2)

capacity at 20 C rate (3400 mA/g) is 55 mAh/g – more than 2 times higher than the capacity obtained for LiFePO₄/C composite.

Although a composite where LiFePO₄/C is uniformly mixed with rGO sheets but does not display any wrapping or anchoring of LiFePO₄/C particles (samples LiFePO₄/C/rGO (2) and (3)) brings slight rate capability improvements, the rGO electron conducting network with this particular grain structure is obviously not efficient enough to lead to significant rate capability improvements.

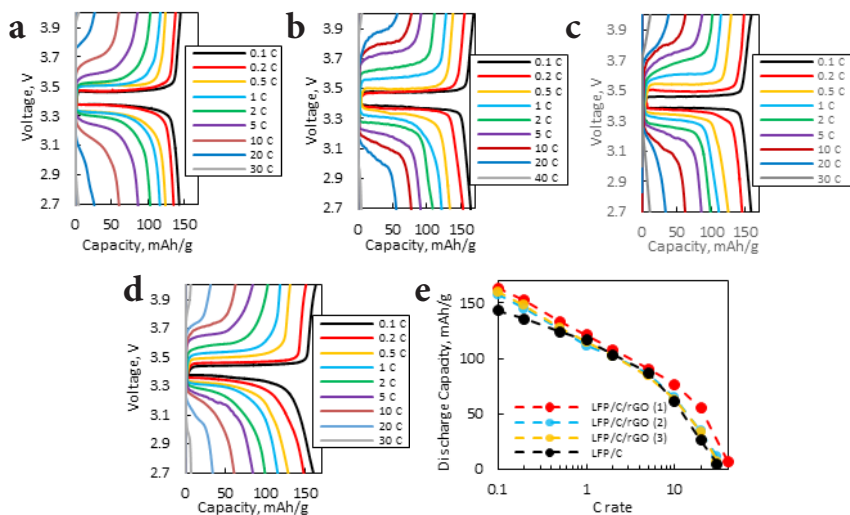


Fig. 4.2. Galvanostatic charge and discharge curves of (a) LiFePO_4/C , (b) $\text{LiFePO}_4/\text{C}/\text{rGO}$ (1), (c) $\text{LiFePO}_4/\text{C}/\text{rGO}$ (2), (d) $\text{LiFePO}_4/\text{C}/\text{rGO}$ (3) and (e) rate capabilities of the obtained composites; 1 C = 170 mA/g

The increase of the galvanostatically measured charge capacities above 5 C rate for rGO containing cathodes is seen due to the electron – conducting network created by rGO in LiFePO_4/C improving the electron transport in the cathode. However, the capacity seems to have increased not only at the higher charge and discharge rates, but also lower rates. For sample $\text{LiFePO}_4/\text{C}/\text{rGO}$ (1) the additional discharge capacity at 0.1 C rate is around 21 mAh/g. Smaller increases can also be observed for other rGO-containing samples.

In order to determine the charge capacity of pure rGO, galvanostatic charge and discharge experiments were also performed on rGO electrodes. rGO charge and discharge curves show that only a small part of the 1050 – 1200 mAh/g charge capacity is obtained between 2.7 V un 4.0 V (see reference [100] for more details). Therefore lithium insertion into rGO layers cannot be the only explanation of the increased low rate capacity of $\text{LiFePO}_4/\text{C}/\text{rGO}$ composites. The increase of the amount of the stored lithium in $\text{LiFePO}_4/\text{C}/\text{rGO}$ (1) and other obtained $\text{LiFePO}_4 - \text{rGO}$ composites is most likely a combination of three phenomena: increased fraction of the electrochemically active LiFePO_4 particles due to the rGO electron-conducting network, chemical bonding of lithium and rGO (lithium insertion in rGO) [9, 101] and lithium storage in $\text{LiFePO}_4/\text{C} - \text{rGO}$ interface as has been observed for a few other composites [90, 102].

4.2. Electrochemical Properties of LiFePO_4 Thin Films

4.2.1. Thin Films Deposited by Pulsed Laser Deposition

The XRD analysis of the prepared PLD target indicates that the material is pristine LiFePO_4 . All peaks correspond to the orthorhombic crystal lattice of LiFePO_4 and Pnma space group. Raman spectroscopy and ICP-OES measurements also confirm that the prepared material is pristine LiFePO_4 .

The XRD data for the obtained LiFePO_4 thin films displays only peaks characteristic LiFePO_4 . ICP-OES results show stoichiometry $\text{Li}_{0.94}\text{Fe}_{1.01}\text{P}_{0.99}\text{O}_{3.96}$, which indicates slight lithium evaporation during the thin film deposition. SIMS indicates a uniform Li, Fe and PO distribution in the bulk of the thin film. XPS data show maxima characteristic to Fe^{2+} and does not indicate any considerable impurities.

The SEM images of the thin films (fig. 4.3.) indicate that the obtained thin films are composed of a longitudinal particles with an average diameter of 5 μm . These particles are composed of smaller grains with diameter of 50–500 nm as shown in fig. 4.3. b. The colour of the grains in fig. 4.3. is different due to variations in the crystallographic orientations. A few cracks can also be observed, they are most likely formed as a result of the substrate heating due to different thermal expansion coefficients of Nb:STO and LiFePO_4 [103–105].

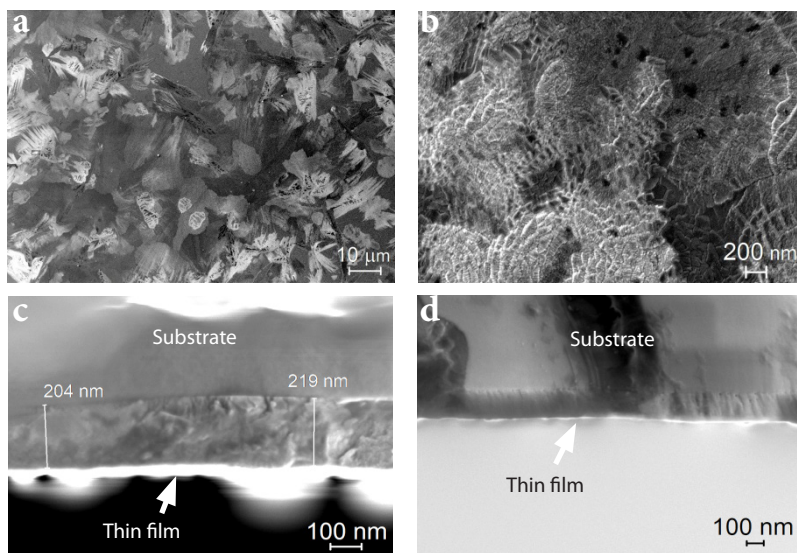


Fig. 4.3. LiFePO_4 thin film SEM (a),(b) surface and (c),(d) cross-section images

Cross-sections of LiFePO_4 thin films can be seen in fig. 4.3. c and d. They indicate that the thin film is dense, with no significant pores and with a rather smooth surface. This is also confirmed by AFM. The analysis of AFM results indicates that the actual surface is only 2 % larger than the projected one. Thin film deposition rate was determined to be 200 nm/h.

The discharge capacities of the obtained thin films are up to 118 mAh/g for the 100 nm thin film (see fig. 4.4.). This constitutes around 70 % of the theoretical capacity of LiFePO_4 , which is 170 mAh/g. The capacities are very high when compared with other studies of LiFePO_4 thin films where no carbon additives have been used [84,106–115]. All electrochemical measurements have been performed in two electrode electrochemical cells that were modified in order to avoid undesired side reactions connected with the electrolyte decomposition. At sufficiently small mass of active material the signal from such side reactions becomes significant.

Obtained LiFePO_4 thin films have a very good cyclability – 85 % of the initial discharge capacity of a 200 nm thin film is retained after 100 charge and discharge cycles at 0.7 C rate (fig. 4.4. e). Cyclic voltammetry (CV) curves display the peaks characteristic to lithium insertion and extraction (fig. 4.4. f).

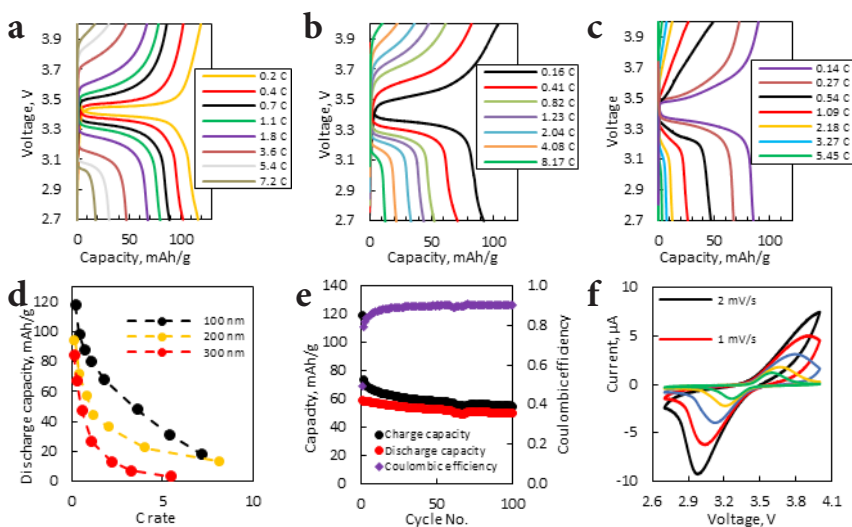


Fig. 4.4. Galvanostatic charge and discharge experiments: (a) 100 nm, (b) 200 nm and (c) 300 nm thick LiFePO_4 thin film charge and discharge curves, (d) rate capabilities, (e) cyclability of a 200 nm thin film, (f) cyclic voltammetry curve, 1 C = 170 mA/g

Electrochemical impedance spectroscopy (EIS) was performed for several LiFePO_4 thin films – see fig. 4.5. Charge transfer resistance increases with

increasing LiFePO_4 thin film thickness, and the values of the charge transfer resistance are close to those of the expected electronic resistance of the thin film.

By using EIS and galvanostatic intermittent titration technique (GITT) the effective chemical diffusion coefficients of LiFePO_4 thin films were determined. Their values can be seen in fig. 4.5. b and c att. For stoichiometries that are close to $\text{Li}_{0.5}\text{FePO}_4$, the effective chemical lithium diffusion coefficient D_{Li} is approximately $1 \cdot 10^{-17}$ cm^2/s . At higher and lower lithium concentrations the determined diffusion coefficients are larger.

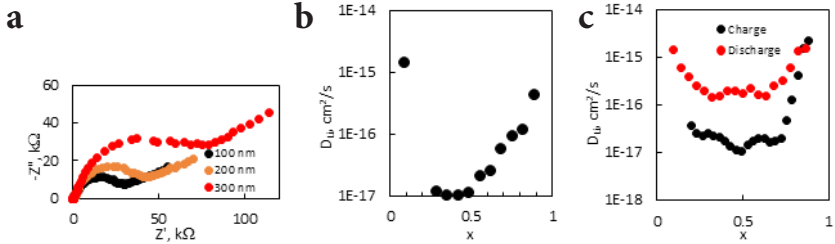


Fig. 4.5. (a) EIS results for LiFePO_4 thin films with various thicknesses; effective chemical lithium diffusion coefficients for a 200 nm LiFePO_4 thin film obtained by using (b) EIS and (c) GITT

The effective chemical diffusion coefficient of lithium calculated from GITT data in intermediate states of charge is approximately 10^{-17} cm^2/s or 10^{-16} cm^2/s for calculations done by using charge and discharge data respectively. The diffusion coefficients calculated from charge and discharge measurements differ because the thin film de-lithiation process has larger resistance (higher overvoltage). This is because thin film was deposited in a stoichiometry that is close to LiFePO_4 (and not FePO_4), therefore during de-lithiation additional mechanical strains can develop.

Diffusion coefficients calculated both from EIS and GITT data are close and are also in agreement with the values determined from the CV curves by using Randles – Sevcik equation (10^{-18} – 10^{-17} cm^2/s).

By interpreting the calculated effective chemical diffusion coefficients one has to take into account that, firstly, the model which is used for calculation of D_{Li} assumes that all particles are lithiating and de-lithiating at the same time, which might not be the case with LiFePO_4 [116]. Secondly, the aforementioned methods for calculating D_{Li} are intended for solid solutions and not for two-phase materials such as LiFePO_4 . Therefore the change in the free energy that comes from the separation of lithium rich and lithium poor phases is not taken into account [117]. Due to aforementioned reasons the calculated results are called effective (or apparent) chemical diffusion coefficients, and they characterize not only the diffusion but also the overall lithium kinetics in the LiFePO_4 electrode.

4.2.2. Thin Films Deposited by Magnetron Sputtering

The XRD data of LiFePO_4 thin films deposited by radio frequency magnetron sputtering confirm that recrystallized thin films are composed of crystalline LiFePO_4 . Fig. 4.6. shows SEM images of LiFePO_4 thin films obtained by magnetron sputtering. Distinct grains can be observed in the thin film with a size of 1 – 10 μm . Although the grains are packed rather densely, grain boundaries can clearly be distinguished. No cracks are formed during the deposition, the surface adhesion is sufficient for the thin film to adhere to the substrate.

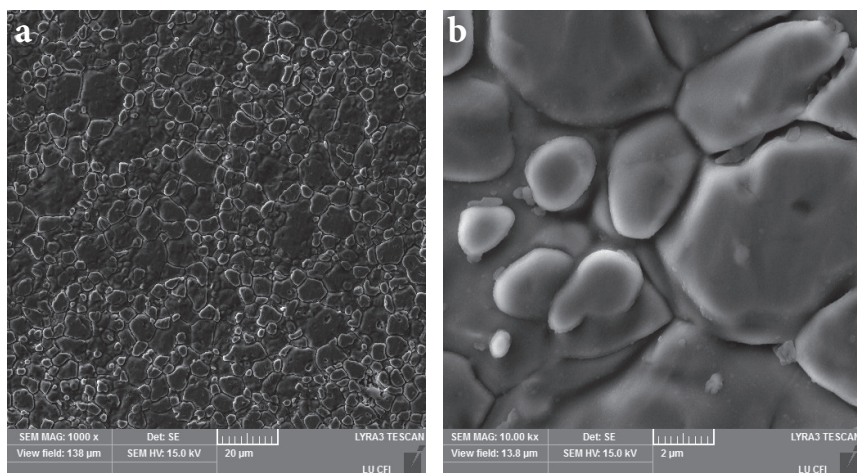


Fig. 4.6. SEM images of LiFePO_4 thin films obtained by magnetron sputtering

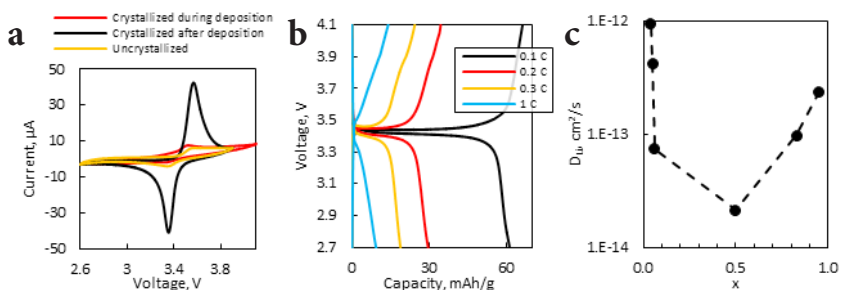


Fig. 4.7. (a) CV curves for various LiFePO_4 thin films ($v = 1 \text{ mV/s}$), (b) galvanostatic charge and discharge curves for 1000 nm thin film, $1 \text{ C} = 170 \text{ mA/g}$, (c) effective chemical diffusion coefficient of lithium in a LiFePO_4 thin film at various states of charge

CV curves in fig. 4.7. a indicate that the best electrochemical properties can be obtained by recrystallizing the thin film after its deposition. Recrystallization is important because the particles reaching the substrate during the deposition may not have sufficient energy to form ordered crystalline structures. The obtained capacities are up to 61 mAh/g at 0.1 C rate (17 mA/g) for a 1000 nm film (see fig. 4.7. b). The capacities measured at higher charge and discharge rates are 30 mAh/g at 0.2 C, 19 mAh/g at 0.3 C and 10 mAh/g at 1 C.

Effective chemical diffusion coefficients of lithium have also been determined for LiFePO_4 thin films deposited by magnetron sputtering – see fig. 4.7. c. The determined diffusion coefficients are several orders of magnitude higher than the ones obtained for thin films deposited by PLD. However, these values are also in agreement with the ones reported in literature (in the range of 10^{-18} to 10^{-10} cm^2/s [12, 82–84]). It must again be noted that the values of effective chemical diffusion coefficients are determined not only by lithium diffusion but also by differences in electrode morphology, grain structure and composition.

4.3. The Analysis of Sequential LiFePO_4 Particle Charging and Discharging

4.3.1. *In-situ XAS Measurements of LiFePO_4 Bulk Material*

LiFePO_4 cathode was charged in order to obtain FePO_4 . The charging was first done in a constant current, then – in constant voltage mode. The current used was 0.27 mA (2 C or 340 mA/g). By charging the LiFePO_4 Fe oxidation state changes from 2+ to 3+ and Fe X-ray absorption K-edge shifts to higher energies. A shift from 7127 eV to 7131 eV can be observed, which is consistent with the results reported in literature [118–123].

The intensity of the X-rays passed through a LiFePO_4 particle at different states of charge (SOC) of the LiFePO_4 electrode can be seen in Fig. 4.8. The LiFePO_4 electrode was first discharged. However, the SOC of the particular LiFePO_4 particle did not change until the electrode was discharged to 65% SOC. For a completely discharged particle Fe^{3+} has changed to Fe^{2+} . By charging the electrode the particle still consisted of mostly Fe^{2+} both at 30 % and 60 % SOC. However, at 60% SOC first indications of the particle being

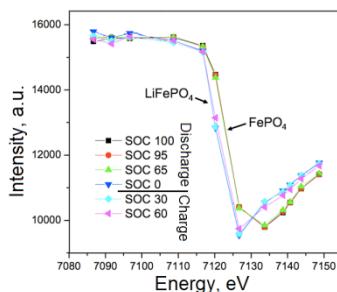


Fig. 4.8. Intensity of the X-rays passed through a LiFePO_4 particle at various electrode SOC

de-lithiated can be observed. The results allow to conclude that the particular LiFePO_4 particle was charged and discharged at a specific SOC of the LiFePO_4 cathode. In the case of the specific LiFePO_4 particle that SOC corresponds to the approximate overall electrode stoichiometry $\text{Li}_{0.5}\text{FePO}_4 - \text{Li}_{0.6}\text{FePO}_4$.

In order to view sequential charging and discharging of LiFePO_4 grains an agglomeration of LiFePO_4 at 35 % SOC was analysed (see fig. 4.9). 7127 eV X-ray energy used to obtain fig. 4.9. a is at the maximum of the Fe^{2+} K-edge. However, it is located before the Fe^{3+} K-edge, therefore Li_xFePO_4 containing mostly Fe^{2+} is darker than the Li_xFePO_4 containing mostly Fe^{3+} . The Fe distribution in the overall image can be evaluated by looking at fig. 4.9. where signal from the same electrode area is shown at pre-edge X-ray energies.

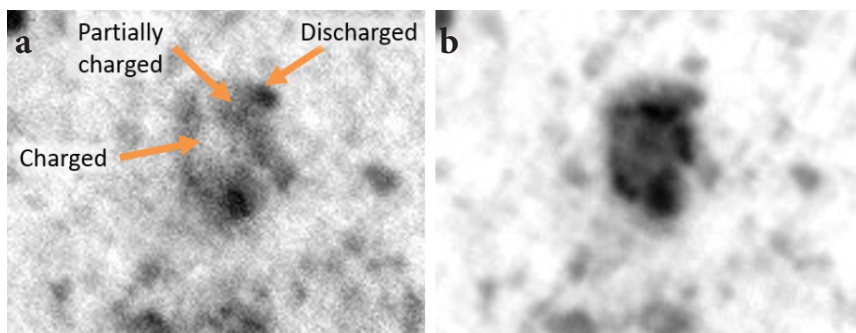


Fig. 4.9. An agglomerate of LiFePO_4 particles at 35 % SOC, X-ray energy: (a) 7127 eV; (b) 7109 eV (pre-edge); at 35% SOC individual grains within a single agglomerate have a different lithium content.

At 35 % SOC charged (darker) and discharged (lighter) LiFePO_4 grains can be observed simultaneously even within a single agglomeration of grains. This observation confirms the sequential LiFePO_4 grain lithiation and de-lithiation. By taking into account that there are several partially charged grains it can be concluded that lithium is being inserted and extracted from several LiFePO_4 grains simultaneously – at a given moment of time there is a specific set or population of grains that are electrochemically active.

For the first time *in-situ* XANES imaging experiments have been performed on a LiFePO_4 cathode. Strong evidence has been obtained for a sequential grain-by-grain charging and discharging of the LiFePO_4 electrode.

4.3.2. Sequential Particle Charging and Discharging in LiFePO_4 Thin Films

Voltage hysteresis measurements were performed for LiFePO_4 thin films deposited by PLD. The measurements are based on a galvanostatic charge and discharge experiments in a limited charge interval. Open circuit voltage

(OCV) is being measured between galvanostatic measurements. Voltage hysteresis measurements were conducted in the characteristic LiFePO_4 two-phase region which corresponds to a stoichiometry Li_xFePO_4 in which $0.1 < x < 0.9$. The experimental procedure is schematically shown in fig. 4.10. The measurement cycle shown in the figure was repeated several times, the low currents used for hysteresis measurements were varied.



Fig. 4.10. Experimental procedure for a single voltage hysteresis measurement cycle

Voltage hysteresis measurements were conducted on four LiFePO_4 thin film samples. Sample LFP-H1 is 100 nm thick, LFP-H2 and LFP-H3 – 200 nm thick, LFP-H3L is the thin film LFP-H3 which has been coated with a 400 nm thick LiPON layer. The electrochemically active mass of the thin films were normalized based on their rate capabilities. Voltage hysteresis graphs and Butler – Volmer type dependence or overvoltage versus current are shown in fig. 4.11.

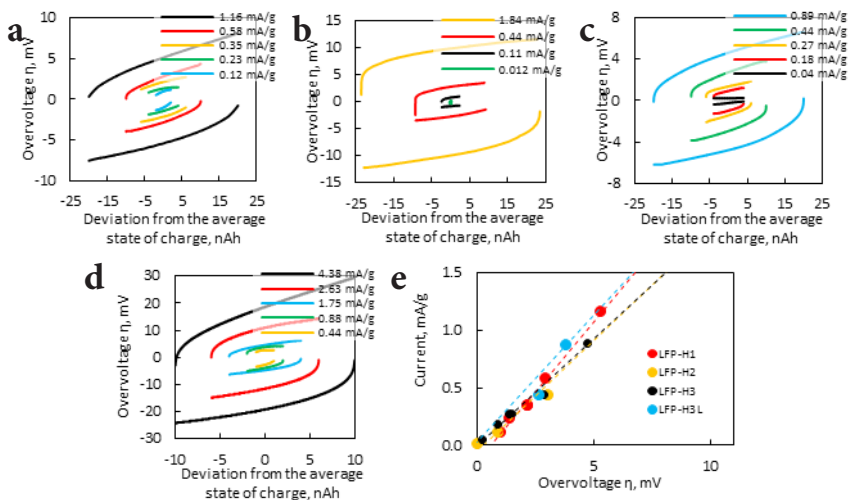


Fig. 4.11.att. Voltage hysteresis obtained at several currents for samples (a) LFP-H1, (b) LFP-H2, (c) LFP-H3, (d) LFP-H3L; (e) Butler – Volmer type dependence between overvoltage and specific currents

The results indicate that if 1–5 % galvanostatic charge and discharge would be performed at intermediate SOC with infinitely low currents, there would be no voltage hysteresis or the observed voltage hysteresis would be extremely small. Even if voltage and current dependence at very small currents cannot be fitted with a linear line, there are still several data points indicating voltage hysteresis bellow 2 mV which is at least an order of magnitude lower than reported in literature for LiFePO_4 bulk material [59].

The results contradict the expectations according to the current model which predicts a non-vanishing voltage hysteresis due to non-monotonic lithium chemical potential – concentration dependence and sequential particle charging and discharging [59]. The disappearance of voltage hysteresis indicates that the sequential charging and discharging of LiFePO_4 particles in thin film can occur in a significantly different way than in bulk material. As the grains in a thin film are tightly connected and they are not separated by a layer of carbon coating or electrolyte, mass transfer between the grains can take place more efficiently. This can influence the way in which lithium is being inserted and extracted from the LiFePO_4 grain. Inner mechanical strains can also play a significant role.

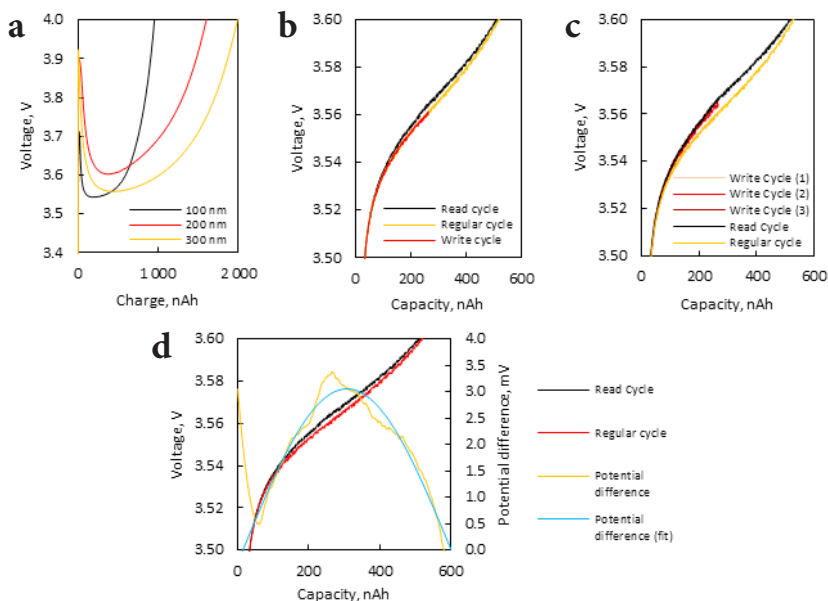


Fig. 4.12. Electrochemical effects observed in LiFePO_4 thin films: (a) a local maximum of the electric potential at the beginning of the charge (200 nA current), (b) and (c) memory effect with one and three write cycles and (d) potential difference due to the memory effect

Two more electrochemical phenomena have been observed for LiFePO_4 thin films. Firstly, at the first galvanostatic charging curve of a LiFePO_4 thin film an uncharacteristically high local electric potential maximum can be observed (see fig. 4.12. a). Secondly, the memory effect has been observed in LiFePO_4 thin film, the results are shown in fig. 4.12. b, c and d. The reader can learn more about the origins of the memory effect in the reference [58].

The most likely explanation for the local maximum of the LiFePO_4 thin film electric potential maximum is simultaneous charging and discharging of LiFePO_4 grains via solid solution mode. However, when the cell reaches a specific overvoltage, irreversible changes at the LiFePO_4 electrode take place. As a result of this it becomes energetically more favourable for lithium rich and lithium poor phases to separate. The aforementioned effect has been observed before in several LiFePO_4 bulk electrodes [58, 86, 124–126]. However, it has never been as pronounced as in LiFePO_4 thin films obtained in this work, and this phenomenon has never been analysed in detail.

Sequential charging and discharging of LiFePO_4 grains or their agglomerations is also confirmed by observing the memory effect (fig. 4.12. b, c and d). The experimental procedure for memory effect measurements is shown in fig. 4.13. The memory effect [58] is based on the fact that during a partial charge and discharge cycle only a part of the electrode is being charged and discharged. After this partial charge and discharge cycle the electrode is in a metastable state which leads to an increased electrode overpotential during a part of the next full charge or discharge. When comparing the results obtained for thin films with those seen for bulk material, the overpotential in the read cycle is more stretched out and not as localized as for bulk electrodes. Nevertheless the existence of the memory effect confirms that sequential grain charging and discharging takes place in LiFePO_4 thin film. However, the changes in electric potential observed during the read cycle in LiFePO_4 thin film are much less pronounced than those observed for bulk material.

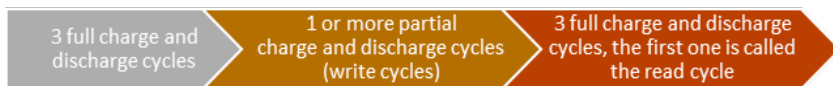


Fig. 4.13. The experimental procedure for memory effect measurements

CONCLUSIONS

By completing the objectives of this work the aim of the work has been achieved – the understanding of the working principles of LiFePO_4 lithium ion battery cathode material has been expanded. The results of this work can be used to increase the rate of lithium insertion and extraction in LiFePO_4 and potentially other two phase lithium insertion and extraction material electrodes. Three main conclusions can be drawn which correspond to the three chapters describing the results of this work.

1. Although $\text{LiFePO}_4/\text{C}/\text{rGO}$ (rGO – reduced graphene oxide) with a remarkably high rate capability when comparing to other $\text{LiFePO}_4/\text{C}/\text{rGO}$ composites [9, 25–34, 127] has been obtained, the main scientific novelty of this part of the work is the conclusions drawn about the optimal $\text{LiFePO}_4/\text{C}/\text{rGO}$ grain structure. The introduction of graphene oxide (GO) at the earliest synthesis stage enables to obtain a grain structure where rGO sheets are wrapped around LiFePO_4 grains and LiFePO_4 particles are anchored on rGO sheets. The electron conducting network created by rGO via this synthesis route enables to achieve the highest charge capacity and rate capability of the $\text{LiFePO}_4/\text{C}/\text{rGO}$ composite. GO added in later synthesis steps creates a grain structure where rGO sheets have been uniformly mixed with LiFePO_4/C but do not necessarily wrap around LiFePO_4 grains. Grain structure in which LiFePO_4 grains have been wrapped in rGO and anchored on it can also improve the charge capacity at low charge and discharge rates. The extra charge capacity of the obtained $\text{LiFePO}_4/\text{C}/\text{rGO}$ can be explained with the electron-conducting network of rGO increasing the fraction of the electrochemically active LiFePO_4 particles, lithium inserting in rGO and lithium storage in LiFePO_4/C – rGO interface. The large charge capacity and rate capability of the obtained $\text{LiFePO}_4/\text{C}/\text{rGO}$ composite makes it suitable for use in advanced lithium ion batteries.
2. High charge capacity LiFePO_4 thin films have been obtained with pulsed laser deposition. Their charge capacity is up to 118 mAh/g which is one of the highest values reported for pristine LiFePO_4 thin films. Due to the two-phase nature of LiFePO_4 and sequential grain charge and discharge the determined effective chemical diffusion coefficient of lithium is the lowest for stoichiometry $\text{Li}_{0.5}\text{FePO}_4$ and is equal to approximately 10^{-17} cm^2/s . At cell voltages close to 2.7 and 4.0 V undesired side reactions take place at the current collector – electrolyte interphase. They are connected with the decomposition of the liquid electrolyte. The methodology of the electrochemical measurements has been improved in order to avoid such

side reactions. Relatively high charge capacity (up to 61 mAh/g) LiFePO_4 thin films can be obtained on a stainless steel substrate via radio frequency magnetron sputtering. This demonstrates the possibility to use this technique for depositing large area LiFePO_4 cathodes which can be used for large area thin film lithium ion batteries.

3. By studying X-ray absorption near edge structure (XANES) of Fe K-edge in LiFePO_4 in imaging mode it was shown that LiFePO_4 grains are charging and discharging sequentially. Even in a single agglomeration lithium rich and lithium poor Li_xFePO_4 particles can be observed. For the first time electrochemical experiments characterizing sequential grain charging and discharging have been performed on LiFePO_4 thin films. The observations of voltage hysteresis and memory effect at low currents were performed. The experimental results show that for LiFePO_4 thin films contrary to the bulk material electrodes nearly vanishing voltage hysteresis can be observed. Although several electrochemical features point to sequential particle-by-particle charging and discharging behaviour, the disappearance of voltage hysteresis means that LiFePO_4 thin film lithiates and de-lithiates in a way that is different from bulk electrode lithiation and de-lithiation. This is associated with the different grain structure of the thin film and indicates that the grain boundaries have a crucial role in LiFePO_4 cathodes. The research done in this work serves as a ground for further improvements of the existing LiFePO_4 particle-by-particle charging and discharging model by taking into account the inter-grain lithium ion and electron transport of LiFePO_4 . In long term these results can serve as a ground for calculation – based way of developing high power LiFePO_4 electrodes and other two phase lithium insertion and extraction material electrodes.

THESES

1. Anchoring LiFePO_4 particles on reduced graphene oxide sheets and wrapping LiFePO_4 grains with reduced graphene oxide sheets are one of the best techniques for improving the rate capability of LiFePO_4 cathodes. LiFePO_4/C – reduced graphene oxide interphase provides additional sites for lithium storage in $\text{LiFePO}_4/\text{C}/\text{rGO}$
2. LiFePO_4 thin films with no additional electron – conducting additives have been deposited by pulsed laser deposition, their charge capacity is close to the capacity of LiFePO_4 bulk material. LiFePO_4 thin films were deposited by magnetron sputtering, they can serve as the cathode for large area thin film lithium ion batteries.
3. Lithium insertion and extraction in Li_xFePO_4 bulk electrode and thin films takes place particle by particle. Nearly vanishing voltage hysteresis has been observed for LiFePO_4 thin film electrode, indicating that there are significant differences in lithium insertion and extraction mechanisms in LiFePO_4 thin films in comparison with the bulk material electrode.

REFERENCES

- [1] A.K. Padhi, K. Nanjundaswamy, J. Goodenough, *J. Electrochem. Soc.* 144 (1997) 1188.
- [2] P.P. Prosini, D. Zane, M. Pasquali, *Electrochim. Acta* 46 (2001) 3517.
- [3] A. Yamada, S.C. Chung, K. Hinokuma, *J. Electrochem. Soc.* 148 (2001) A224.
- [4] A.S. Andersson, *Electrochem. Solid-State Lett.* 3 (1999) 66.
- [5] M. Takahashi, H. Ohtsuka, K. Akuto, Y. Sakurai, *J. Electrochem. Soc.* 152 (2005) A899.
- [6] T. Maxisch, G. Ceder, *Phys. Rev. B* 73 (2006) 174112.
- [7] R. Malik, A. Abdellahi, G. Ceder, *J. Electrochem. Soc.* 160 (2013) A3179.
- [8] R. Tian, G. Liu, H. Liu, L. Zhang, X. Gu, Y. Guo, H. Wang, L. Sun, W. Chu, *RSC Adv.* 5 (2015) 1859.
- [9] B. Lung-Hao Hu, F.-Y. Wu, C.-T. Lin, A.N. Khlobystov, L.-J. Li, *Nat. Commun.* 4 (2013) 1687.
- [10] J. Wang, X. Sun, *Energy Environ. Sci.* 8 (2015) 1110.
- [11] K. Zaghbi, A. Guerfi, P. Hovington, A. Vjih, M. Trudeau, A. Mauger, J.B. Goodenough, C.M. Julien, *J. Power Sources* 232 (2013) 357.
- [12] P.P. Prosini, M. Lisi, D. Zane, M. Pasquali, *Solid State Ionics* 148 (2002) 45.
- [13] S. Shi, L. Liu, C. Ouyang, D. Wang, Z. Wang, L. Chen, X. Huang, *Phys. Rev. B* 68 (2003) 195108.
- [14] R. Amin, J. Maier, P. Balaya, D.P. Chen, C.T. Lin, *Solid State Ionics* 179 (2008) 1683.
- [15] Z. Zhang, C. Qu, M. Jia, Y. Lai, J. Li, *J. Cent. South Univ.* 21 (2014) 2604.
- [16] J. Li, B.L. Armstrong, C. Daniel, J. Kiggans, D.L. Wood, *J. Colloid Interface Sci.* 405 (2013) 118.
- [17] O. Toprakci, L. Ji, Z. Lin, H.A.K. Toprakci, X. Zhang, *J. Power Sources* 196 (2011) 7692.
- [18] C.Y. Wu, G.S. Cao, H.M. Yu, J. Xie, X.B. Zhao, *J. Phys. Chem. C* 115 (2011) 23090.
- [19] M.M. Doeff, Y. Hu, F. McLarnon, R. Kostecki, *Electrochem. Solid-State Lett.* 6 (2003) A207.
- [20] B. Jin, E.M. Jin, K.-H. Park, H.-B. Gu, *Electrochem. Commun.* 10 (2008) 1537.
- [21] X. Sun, J. Li, C. Shi, Z. Wang, E. Liu, C. He, X. Du, N. Zhao, *J. Power Sources* 220 (2012) 264.
- [22] L. Kavan, R. Bacsá, M. Tunckol, P. Serp, S.M. Zakeeruddin, F. Le Formal, M. Zúkalová, M. Graetzel, F. Formal, *J. Power Sources* 195 (2010) 5360.
- [23] K.S. Novoselov, A.K. Geim, S.V. Morozov, D. Jiang, Y. Zhang, S.V. Dubonos, I.V. Grigorieva, A.A. Firsov, *Science* 306 (2004) 666.
- [24] D.R. Cooper, B. D'Anjou, N. Ghattamaneni, B. Harack, M. Hilke, A. Horth, N. Majlis, M. Massicotte, L. Vandsburger, E. Whiteway, V. Yu, *ISRN Condens. Matter Phys.* 2012 (2012).
- [25] C. Su, X. Bu, L. Xu, J. Liu, C. Zhang, *Electrochim. Acta* 64 (2012) 190.
- [26] J. Yang, J. Wang, D. Wang, X. Li, D. Geng, G. Liang, M. Gauthier, R. Li, X. Sun, *J. Power Sources* 208 (2012) 340.
- [27] Y. Zhang, W. Wang, P. Li, Y. Fu, X. Ma, *J. Power Sources* 210 (2012) 47.
- [28] Y. Tang, F. Huang, H. Bi, Z. Liu, D. Wan, *J. Power Sources* 203 (2012) 130.
- [29] H. Xu, J. Chang, J. Sun, L. Gao, *Mater. Lett.* 83 (2012) 27.
- [30] L. Wang, H. Wang, Z. Liu, C. Xiao, S. Dong, P. Han, Z. Zhang, X. Zhang, C. Bi, G. Cui, *Solid State Ionics* 181 (2010) 1685.
- [31] X. Zhou, F. Wang, Y. Zhu, Z. Liu, *J. Mater. Chem.* 21 (2011) 3353.
- [32] Y. Ding, Y. Jiang, F. Xu, J. Yin, H. Ren, Q. Zhuo, Z. Long, P. Zhang, *Electrochem. Commun.* 12 (2010) 10.
- [33] Y. Wang, Z.-S. Feng, J.-J. Chen, C. Zhang, *Mater. Lett.* 71 (2012) 54.

- [34] O. Toprakci, H.A.K. Toprakci, L. Ji, Z. Lin, R. Gu, X. Zhang, *J. Renew. Sustain. Energy* 4 (2012) 013121.
- [35] F.-Y. Su, C. You, Y.-B. He, W. Lv, W. Cui, F. Jin, B. Li, Q.-H. Yang, F. Kang, *J. Mater. Chem.* 20 (2010) 9644.
- [36] H. Wang, Y. Yang, Y. Liang, L.-F. Cui, H.S. Casalongue, Y. Li, G. Hong, Y. Cui, H. Dai, *Angew. Chem. Int. Ed. Engl.* 50 (2011) 7364.
- [37] J.-G. Kim, H.-K. Kim, J.-P. Jegal, K.-H. Kim, J.-Y. Kim, S.-H. Park, K.-B. Kim, *Proc. Int. Conf. Nanomater. Appl. Prop.* (2012) 3.
- [38] S.-M. Bak, K. Nam, C. Lee, K.-B.K.-H. Kim, H. Jung, X.-Q. Yang, *J. Mater. Chem.* 21 (2011) 17309.
- [39] W. Zhang, Y. Zeng, C. Xu, N. Xiao, Y. Gao, L.-J. Li, X. Chen, H.H. Hng, Q. Yan, *Beilstein J. Nanotechnol.* 3 (2012) 513.
- [40] X. Rui, D. Sim, K. Wong, J. Zhu, W. Liu, C. Xu, H. Tan, N. Xiao, H.H. Hng, T.M. Lim, Q. Yan, *J. Power Sources* 214 (2012) 171.
- [41] Y. Jiang, W. Xu, D. Chen, Z. Jiao, H. Zhang, Q. Ma, X. Cai, B. Zhao, Y. Chu, *Electrochim. Acta* 85 (2012) 377.
- [42] H. Liu, G. Yang, X. Zhang, P. Gao, L. Wang, J. Fang, J. Pinto, X. Jiang, *J. Mater. Chem.* 22 (2012) 11039.
- [43] J. Zhu, R. Yang, K. Wu, *Ionics (Kiel)*. 0 (2012) Available only online.
- [44] H. Liu, P. Gao, J. Fang, G. Yang, *Chem. Commun. (Camb)*. 47 (2011) 9110.
- [45] G. Kucinskis, G. Bajars, J. Kleperis, *J. Power Sources* 240 (2013) 66.
- [46] F.-Y. Su, Y.-B. He, B. Li, X.-C. Chen, C.-H. You, W. Wei, W. Lv, Q.-H. Yang, F. Kang, *Nano Energy* 1 (2012) 429.
- [47] P. Bai, D.A. Cogswell, M.Z. Bazant, *Nano Lett.* 11 (2011) 4890.
- [48] K. Weichert, W. Sigle, P. a van Aken, J. Jamnik, C. Zhu, R. Amin, T. Acartürk, U. Starke, *J. Maier, J. Am. Chem. Soc.* 134 (2012) 2988.
- [49] C. Delacourt, P. Poizot, J.-M. Tarascon, C. Masquelier, *Nat. Mater.* 4 (2005) 254.
- [50] J.L. Dodd, R. Yazami, B. Fultz, *Electrochem. Solid-State Lett.* 9 (2006) A151.
- [51] F. Zhou, T. Maxisch, G. Ceder, *Phys. Rev. Lett.* 97 (2006) 155704.
- [52] A.S. Andersson, J.O. Thomas, *J. Power Sources* 97-98 (2001) 498.
- [53] C. Delmas, M. Maccario, L. Croguennec, F. Le Cras, F. Weill, *Nat. Mater.* 7 (2008) 665.
- [54] G. Brunetti, D. Robert, P. Bayle-Guillemaud, J.L. Rouvière, E.F. Rauch, J.F. Martin, J.F. Colin, F. Bertin, C. Cayron, *Chem. Mater.* 23 (2011) 4515.
- [55] L. Gu, C. Zhu, H. Li, Y. Yu, C. Li, S. Tsukimoto, J. Maier, Y. Ikuhara, *J. Am. Chem. Soc.* 133 (2011) 4661.
- [56] Y. Sun, X. Lu, R. Xiao, H. Li, X. Huang, *Chem. Mater.* 24 (2012) 4693.
- [57] M.E. Schuster, D. Teschner, J. Popovic, N. Ohmer, F. Girgsdies, J. Törnøw, M.G. Willinger, D. Samuelis, M.-M. Titirici, J. Maier, R. Schlögl, *Chem. Mater.* 26 (2014) 1040.
- [58] T. Sasaki, Y. Ukyo, P. Novák, *Nat. Mater.* 12 (2013) 569.
- [59] W. Dreyer, J. Jamnik, C. Gühllke, R. Huth, J. Moskon, M. Gaberscek, *Nat. Mater.* 9 (2010) 448.
- [60] J. Moskon, J. Jamnik, M. Gaberscek, *Solid State Ionics* 238 (2013) 24.
- [61] M.A. Roscher, O. Bohlen, J. Vetter, *Int. J. Electrochem.* 2011 (2011) 1.
- [62] C. Zhu, *Size Effects on Lithium Storage and Phase Transition in LiFePO₄/FePO₄ System*, University of Stuttgart, 2013.
- [63] C. Zhu, L. Gu, L. Suo, J. Popovic, H. Li, Y. Ikuhara, J. Maier, *Adv. Funct. Mater.* 24 (2014) 312.
- [64] A. Patil, V. Patil, D. Wook Shin, J.-W. Choi, D.-S. Paik, S.-J. Yoon, *Mater. Res. Bull.* 43 (2008) 1913.

- [65] Y. Yang, Z. Peng, G. Wang, G. Ruan, X. Fan, L. Li, H. Fei, R.H. Hauge, J.M. Tour, ACS Nano 8 (2014) 7279.
- [66] N.J. Dudney, Mater. Sci. Eng. B 116 (2005) 245.
- [67] Y. Wang, B. Liu, Q. Li, S. Cartmell, S. Ferrara, Z. Daniel, J. Xiao, J. Power Sources 286 (2015) 330.
- [68] D. Linden, T.B. Reddy, Handbook of Batteries, 3rd Edition, McGraw-Hill, 2002.
- [69] M. Thomas, P. Bruce, J. Goodenough, Solid State Ionics 17 (1985) 13.
- [70] M.M. Thackeray, W.I.F. David, P.G. Bruce, J.B. Goodenough, Mater. Res. Bull. 18 (1983) 461.
- [71] K. Mizushima, P. Jones, P. Wiseman, J. Goodenough, Solid State Ionics 3-4 (1981) 171.
- [72] Y. Nishi, J. Power Sources 100 (2001) 101.
- [73] R. Van Noorden, Nature 507 (2014) 26.
- [74] K.A. Kiehne, Battery Technology Handbook, Marcel Dekker, Inc., 2003.
- [75] M. Hu, X. Pang, Z. Zhou, J. Power Sources 237 (2013) 229.
- [76] J. Chen, Materials (Basel). 6 (2013) 156.
- [77] J.B. Goodenough, K.-S. Park, J. Am. Chem. Soc. 135 (2013) 1167.
- [78] B. Xu, D. Qian, Z. Wang, Y.S. Meng, Mater. Sci. Eng. R Reports 73 (2012) 51.
- [79] R. Huggins, Advanced Batteries, Springer, 2009.
- [80] J. Xu, S. Dou, H. Liu, L. Dai, Nano Energy 2 (2013) 439.
- [81] Y. Zhang, C.-Y. Wang, X. Tang, J. Power Sources 196 (2011) 1513.
- [82] A.V. Churikov, A.V. Ivanishchev, I.A. Ivanishcheva, V.O. Sycheva, N.R. Khasanova, E.V. Antipov, Electrochim. Acta 55 (2010) 2939.
- [83] G. Bajars, G. Kucinskis, J. Smits, J. Kleperis, A. Lulis, IOP Conf. Ser. Mater. Sci. Eng. 38 (2012) 012019.
- [84] K. Tang, X. Yu, J. Sun, H. Li, X. Huang, Electrochim. Acta 56 (2011) 4869.
- [85] M. Gaberscek, R. Dominko, J. Jamnik, Electrochem. Commun. 9 (2007) 2778.
- [86] B. Kang, G. Ceder, Nature 458 (2009) 190.
- [87] X. Zhang, H. Guo, X. Li, Z. Wang, L. Wu, Solid State Ionics 212 (2012) 106.
- [88] N. Amdouni, K. Zaghbi, F. Gendron, A. Mauger, C.M. Julien, Ionics (Kiel). 12 (2006) 117.
- [89] N. Meethong, H.-Y.S. Huang, W.C. Carter, Y.-M. Chiang, Electrochem. Solid-State Lett. 10 (2007) A134.
- [90] J. Jamnik, J. Maier, Phys. Chem. Chem. Phys. 5 (2003) 5215.
- [91] K.T. Lee, W.H. Kan, L.F. Nazar, J. Am. Chem. Soc. 131 (2009) 6044.
- [92] V. Srinivasan, J. Newman, Electrochem. Solid-State Lett. 9 (2006) A110.
- [93] H. Matsui, T. Nakamura, Y. Kobayashi, M. Tabuchi, Y. Yamada, J. Power Sources 195 (2010) 6879.
- [94] K. Wasa, M. Kitabatake, H. Adachi, Thin Film Materials Technology, Sputtering of Compound Materials, William Andrew, Inc., 2004.
- [95] M. Ohring, Materials Science of Thin Films, Elsevier, 2002.
- [96] W. Görner, M.P. Hentschel, B.R. Müller, H. Riesemeier, M. Krumrey, G. Ulm, W. Diete, U. Klein, R. Frahm, Nucl. Instruments Methods Phys. Res. Sect. A Accel. Spectrometers, Detect. Assoc. Equip. 467-468 (2001) 703.
- [97] A. Rack, S. Zabler, B.R. Müller, H. Riesemeier, G. Weidemann, A. Lange, J. Goebbels, M. Hentschel, W. Görner, Nucl. Instruments Methods Phys. Res. Sect. A Accel. Spectrometers, Detect. Assoc. Equip. 586 (2008) 327.
- [98] J.H. Warner, F. Schaffel, M. Rummeli, A. Bachmatiuk, Graphene: Fundamentals and Emergent Applications, 1st ed., Elsevier, 2012.
- [99] J.D. Stoll, A. Kolmakov, Nanotechnology 23 (2012) 505704.

- [100] K. Kaprans, G. Bajars, G. Kucinskis, A. Dorondo, J. Mateuss, J. Gabrusenoks, J. Kleperis, A. Lusis, *IOP Conf. Ser. Mater. Sci. Eng.* 77 (2015) 012042.
- [101] R. Mukherjee, A. V Thomas, D. Datta, E. Singh, J. Li, O. Eksik, V.B. Shenoy, N. Koratkar, *Nat. Commun.* 5 (2014) 3710.
- [102] J. Maier, *Nat. Mater.* 4 (2005) 805.
- [103] D.E. McCready, Y. Liang, V. Shutthanandan, C.M. Wang, S. Thevuthasan, *Adv. X-Ray Anal.* ISSN 1097- (2006) 175.
- [104] D. de Ligny, P. Richet, *Phys. Rev. B* 53 (1996) 3013.
- [105] Z. Chen, Y. Ren, Y. Qin, H. Wu, S. Ma, J. Ren, X. He, Y.-K. Sun, K. Amine, *J. Mater. Chem.* 21 (2011) 5604.
- [106] V. Palomares, I. Ruiz de Larramendi, J. Alonso, M. Bengoechea, a. Goñi, O. Miguel, T. Rojo, *Appl. Surf. Sci.* 256 (2010) 2563.
- [107] M. Köhler, F. Berkemeier, T. Gallasch, G. Schmitz, *J. Power Sources* 236 (2013) 61.
- [108] K.-F. Chiu, *J. Electrochem. Soc.* 154 (2007) A129.
- [109] J. Hong, C. Wang, N.J. Dudney, M.J. Lance, *J. Electrochem. Soc.* 154 (2007) A805.
- [110] J. Xie, N. Imanishi, T. Zhang, A. Hirano, Y. Takeda, O. Yamamoto, *Electrochim. Acta* 54 (2009) 4631.
- [111] X.-J. Zhu, L.-B. Cheng, C.-G. Wang, Z.-P. Guo, P. Zhang, G.-D. Du, H.-K. Liu, *J. Phys. Chem. C* 113 (2009) 14518.
- [112] Z.G. Lu, M.F. Lo, C.Y. Chung, *J. Phys. Chem. C* 112 (2008) 7069.
- [113] F. Sauvage, E. Baudrin, L. Gengembre, J. Tarascon, *Solid State Ionics* 176 (2005) 1869.
- [114] C. Yada, Y. Iriyama, S.-K. Jeong, T. Abe, M. Inaba, Z. Ogumi, *J. Power Sources* 146 (2005) 559.
- [115] S.-W. Song, R.P. Reade, R. Kostecki, K.A. Striebel, *J. Electrochem. Soc.* 153 (2006) A12.
- [116] Y. Li, F. El Gabaly, T.R. Ferguson, R.B. Smith, N.C. Bartelt, J.D. Sugar, K.R. Fenton, D.A. Cogswell, A.L.D. Kilcoyne, T. Tyliszczak, M.Z. Bazant, W.C. Chueh, *Nat. Mater.* (2014).
- [117] Y. Zhu, C. Wang, *J. Phys. Chem. C* 114 (2010) 2830.
- [118] A. Deb, U. Bergmann, S.P. Cramer, E.J. Cairns, *Electrochim. Acta* 50 (2005) 5200.
- [119] C.T. Love, A. Korovina, C.J. Patridge, K.E. Swider-Lyons, M.E. Twigg, D.E. Ramaker, *J. Electrochem. Soc.* 160 (2013) A3153.
- [120] A. Deb, U. Bergmann, E.J. Cairns, S.P. Cramer, *J. Synchrotron Radiat.* 11 (2004) 497.
- [121] A. Deb, U. Bergmann, E.J. Cairns, S.P. Cramer, *J. Phys. Chem. B* 108 (2004) 7046.
- [122] M. Giorgetti, M. Berrettoni, S. Scaccia, S. Passerini, *Inorg. Chem.* 45 (2006) 2750.
- [123] C.-W. Hu, T.-Y. Chen, K.-S. Shih, P.-J. Wu, H.-C. Su, C.-Y. Chiang, A.-F. Huang, H.-W. Hsieh, C.-C. Chang, B.-Y. Shew, C.-H. Lee, *J. Power Sources* 270 (2014) 449.
- [124] W. Shang, L. Kong, X. Ji, *Solid State Sci.* 38 (2014) 79.
- [125] J. Li, J. Wu, Y. Wang, G. Liu, C. Chen, H. Liu, *Mater. Lett.* 136 (2014) 282.
- [126] K.M. Kim, Y.-G. Lee, K.-Y. Kang, Y.S. Yang, J. Kim, *RSC Adv.* 2 (2012) 3844.
- [127] J. Yang, J. Wang, Y. Tang, D. Wang, X. Li, Y. Hu, R. Li, G. Liang, T.-K. Sham, X. Sun, *Energy Environ. Sci.* 6 (2013) 1521.

APPROBATION OF THE WORK

Scientific Projects

This work is connected with the execution of the following scientific projects:

- Latvian Council of Science, cooperation project “Synthesis and studies on controlled porosity composite thin layers and systems for energy storage and conversion applications“, project No. 666/2014 (2014 – 2018),
- Taiwanese – Latvian – Lithuanian scientific cooperation project “Materials and processing development for advanced Li ion batteries” (2012 – 2014)
- National Research Program in Material science (2010 – 2014)

Scientific Conferences

International Conferences

- **G.Kucinskis, G.Bajars, K.Bikova, A.Dindune, J.Ronis, D.Valdniece, J.Kleperis** (25-29/06/2014) Preparation and characterization of LiFePO_4 thin films deposited by RF magnetron sputtering, *11th International Symposium on Systems with Fast Ionic Transport*, Gdansk, Poland, Book of Abstracts: p. 61.
- **G.Kucinskis, G.Bajars, J.Kleperis** (01-04/10/2012) LiFePO_4 cathode for thin film lithium ion batteries, *COST action MP1004 Think Tank meeting*, Kayseri, Turkey
- **G.Kucinskis, G.Bajars, J.Kleperis** (27-31/08/2012) Electrochemical analysis of $\text{Li}_2\text{FeSiO}_4$ cathode material for Li-ion batteries, *14th International Conference – School “Advanced Materials and Technologies”*, Palanga, Lithuania, Book of Abstracts: p. 140.
- **G.Kucinskis, G.Bajars, J.Kleperis, A.Lusis, A.Dindune, Z.Kanepe, J.Ronis** (01-04/07/2012) Preparation and electrochemical properties of $\text{Li}_2\text{FeSiO}_4$ Bulk Material and Thin Films, *10th International Symposium on Systems with Fast Ionic Transport*, Chernogolovka, Russia, Book of Abstracts: p. 76.
- **G.Kucinskis, G.Bajars, J.Kleperis, A.Dindune, Z.Kanepe, J.Ronis** (17-20/04/2012) Synthesis and Electrochemical Performance of $\text{Li}_2\text{FeSiO}_4$ Cathode Material for Lithium Ion Batteries, *International conference on Functional materials and nanotechnologies*. Institute of Solid State Physics, University of Latvia, Riga, Book of abstracts: p. 162.
- **G.Kucinskis, G.Bajars, J.Kleperis, L.Grinberga** (15-18/04/2012) Structure and electrochemical performance of $\text{Li}_2\text{FeSiO}_4$, *10th Spring Meeting of ISE*. Perth, Australia, Book of Abstracts: p.113.

- **G.Kucinskis, J.Smits, L.Grinberga, G.Bajars, J.Kleperis** (22-24/11/2010) Physical and electrochemical characteristics of LiFePO₄/C thin film cathode material for lithium-ion batteries. *6th Russian conference on Physical problems of hydrogen energetics*, St.Petersburg, Russia, Book of Abstracts: p. 167-168.
- **G.Kucinskis, G.Bajars, J.Kleperis, A.Lusis, J.Smits** (01-04/07/2010) Kinetic Characteristics of LiFePO₄/C Thin Films, *9th International Symposium on Systems with Fast Ionic Transport*, Riga, Latvia, Book of Abstracts: p. 123.

Local Conferences

- **G.Kučinskis, G.Bajārs, J.Kleperis** (24-26/02/2015) Voltage Hysteresis of LiFePO₄ Lithium Ion Battery Cathode Material. *ISSP UL 31st Scientific Conference*, Riga, Latvia, Book of abstracts: p. 74.
- **G.Kucinskis, K.Bikova, G.Bajārs, J.Kleperis** (19-21/02/2014) Synthesis and Electrochemical Properties of LiFePO₄/Graphene nanocomposite. *ISSP UL 30th Scientific Conference*, Riga, Latvia, Book of abstracts: p. 96.
- **G.Kucinskis, G.Bajārs, J.Kleperis, K.Bikova** (20-22/02/2013) LiFePO₄/Graphene Nanocomposite Cathode for Lithium Ion Batteries. *ISSP UL 29th Scientific Conference*, Riga, Latvia, Book of abstracts: p. 93.
- **G.Kucinskis, G.Bajars, J.Smits, J.Kleperis** (14-16/02/2011) Comparison of LiFePO₄ Thin Film and Bulk Material Morphology and Electrochemical Properties. *ISSP UL 27th Scientific Conference*, Riga, Latvia, Book of abstracts: p. 31.
- **G.Kučinskis, J.Smits, G.Bajars, J.Kleperis, G.Cikvaidze** (17-19/02/2010) Investigation of Structure and Impedance of Lithium Iron Phosphate, *ISSP UL 26th Scientific Conference*, Riga, Latvia, Book of abstracts: p. 80.

Scientific Schools

- Participation and presenting a poster “Deposition and electrochemical characterization of LiFePO₄ thin films” in a training school „São Paulo School of Advanced Sciences on Electrochemistry, Energy Conversion and Storage (SPASECS)” (07-15/12/2013), Sao Paulo, Brazil.
- Participation in COST Action MP1106 training school “Smart and Green Interfaces – from single bubbles and drops to industrial, environmental and biomedical applications” (23-25/05/2013), Enschede, Netherlands.

Scientific Publications

SCI Publications

- **K.Kaprans, G.Bajars, G.Kucinskis, A.Dorondo, J.Mateuss, J.Gabrusenoks, J.Kleperis, A.Lusis** (2015) Electrophoretic Nanocrystalline Graphene Film Electrode for Lithium ion Battery. *IOP Conference Series: Materials Science and Engineering*, vol. 77, 5 pages (012042)
- **G.Kucinskis, G.Bajars, J.Kleperis** (2013) Graphene in Lithium ion Battery Cathode Materials: A review. *Journal of Power Sources*, vol. 240, 14 pages (p. 66-79)
- **G.Bajars, G.Kucinskis, J.Smits, J.Kleperis, A.Lusis** (2012) Characterization of LiFePO_4/C Composite Thin Films Using Electrochemical Impedance Spectroscopy. *IOP Conference Series: Material Sciences and Engineering*, vol.38, 5 pages (012019)
- **G.Bajars, G.Kucinskis, J.Smits, J.Kleperis** (2011) Physical and Electrochemical Properties of LiFePO_4/C Thin Films Deposited by DC and RF Magnetron Sputtering. *Solid State Ionics*, vol.188, 5 pages (p. 156-159)
- **J.Smits, G.Kucinskis, G.Bajars, J.Kleperis** (2011) Structure and Electrochemical Characteristics of LiFePO_4 as Cathode Material for Lithium-Ion Batteries. *Latvian Journal of Physics and Technical Sciences*, vol. 48, Nr. 2, 4 pages (p. 27-31)

Other Publications

- **G.Kucinskis, G.Bajars, J.Kleperis** (2012) Electrochemical Properties of LiFePO_4 Thin Films Prepared by RF Magnetron Sputtering. *International Scientific Journal for Alternative Energy and Ecology*, # 9, 6 pages

ACKNOWLEDGEMENTS

I express my deepest gratitude to my supervisor, Dr. Gunārs Bajārs, head of Laboratory of Solid State Ionics and lead researcher at ISSP UL, for supervising my thesis and giving valuable advice on analysing and interpreting the data. I also acknowledge Jānis Kleperis, head of Laboratory of Hydrogen Energy Materials and lead researcher at ISSP UL, for valuable advice regarding the analysis of the results. The help of Andrejs Lūsis, the head of the Department of Semiconductor Materials at ISSP UL is also greatly acknowledged.

I am grateful to my colleagues at ISSP UL, especially Kārlis Kundziņš for SEM measurements, Reinis Ignatāns and Aija Plaude for XRD measurements, Jevgēņijs Gabrusenoks and Aleksejs Kuzmins for Raman spectroscopy measurements, Jānis Balodis for the help with magnetron sputtering, Vladimirs Ņemcevs, Mārtiņš Vanags and Artūrs Gruduls for their help with non-standard technical solutions, Jānis Straumēns, Leonīds Birjāns and Vladimirs Ivanovs for helping to make non-standard experimental devices, Jānis Maniks and Roberts Zabels for AFM measurements. Huge thanks also to the other colleagues of the Laboratory of Solid State Ionics and Laboratory of Hydrogen Energy Materials, ISSP UL.

I acknowledge Sidrabe Inc. for allowing to use their magnetron sputtering equipment. The help of Edmunds Mačevskis and Viktors Kozlovs is also acknowledged.

I am deeply grateful to Prof. Joachim Maier, Dr. Dominik Samuelis and other colleagues at Max Planck Institute for Solid State Research in Stuttgart, Germany. Enormous thanks to Nils Ohmer and Chia-Chin Chen. I also thank to all the colleagues at Max Planck Institute for Solid State Research in Stuttgart who helped with advanced sample characterization and creative technological solutions.